Magnetic and Structural Investigations of Nanocrystalline Cobalt-Ferrite

I. Sharifi[1,2], H. Shokrollahi[1]

Abstract

Cobalt ferrite is an important magnetic material due to their large magneto-crystalline anisotropy, high cohercivity, moderate saturation magnetization and chemical stability.In this study, cobalt ferrites Nanoparticles have been synthesized by the co-precipitation method and a new microemulsion route. We examined the cation occupancy in the spinel structure based on the “Rietveld with energies” method. The X-ray measurements revealed the production of a broad single ferrite cubic phase with the average particle sizes of about 12 nm and 7nm, for co-precipitation and micro-emulsion methods, respectively. The FTIR measurements between 400 and 4000 cm^{-1} confirmed the intrinsic cation vibrations of the spinelstructure for the two methods. Furthermore, the Vibrating Sample Magnetometer (VSM) was carried out at room temperature to study the structural and magnetic properties. The results revealed that by changing the method from co-precipitation to the reverse micelle the material exhibits a softer magnetic behavior in such a way that both saturation magnetization and coercivity decrease from 58 to 29 emu/g and from 286 to 25 Oe, respectively.

Keywords: Cobalt ferrite; Magnetic nanoparticles; co-precipitation; micro-emulsion

1. Introduction

The subjects of magnetic materials are quite old and well-studied [1, 2]. Yet they have been rejuvenated in recent years in the context of biomedical application including magnetic resonance imaging (MRI), magnetic fluid hyperthermia (MFH), magnetic separations, biosensors, targeted and controlled drug delivery [3, 4]. Among magnetic materials, magnetic ceramics have been paid special attention due to chemical stability as well as high electrical resistivity. One of the most important magnetic ceramics is spinel ferrites [5, 6]. Among spinel ferrites, $CoFe_2O_4$ has considerably attracted because of their large magneto-crystalline anisotropy, high coercivity, moderate saturation magnetization, large magneto-strictive coefficient, chemical stability and mechanical hardness [7].

$CoFe_2O_4$ has an inverse spinel structure, where oxygen atoms constitute an face center cubic (FCC) lattice and one half of Fe(III) ions occupies the tetrahedral “A” site and the other half, together with Co(II)ions is located on the octahedral “B” site. The different processing methods [8, 9] can be influence the occupation of the tetrahedral and octahedral sites [8-13]. Although the chemical precipitation route is the most widely used process for the synthesis of the magnetic nano-crystals with high simplicity and good grain size control, it leads to the precipitation of the nano-crystals with a relatively broad size distribution [14]. In contrast, the nano-crystals prepared by the micro emulsion method are generally very fine, and shape controlled as compared to those synthesized by other processes with narrow size distribution [15-17]. This paper investigates the effect of site occupancy and particle size in two widely used chemical methods, including co-precipitation and reverse micelles micro emulsion methods on the magnetic and structural properties of cobalt ferrite.

1- Electroceramics Group, Materials Science and Engineering Department, Shiraz University of Technology, 71555-313, Shiraz, Iran, Shokrollahi@sutech.ac.ir
2- Materials and Energy Research Center (MERC), PO Box 31787-316, Karaj, Iran, I.Sharifi@merc.ac.ir

Corresponding author:
I. Sharifi, Electroceramics Group, Materials Science and Engineering Department, Shiraz University of Technology, 71555-313, Shiraz, Iran,
Email: Shokrollahi@sutech.ac.ir

2. Experimental method

2.1. Materials

All chemical reagents− ferric chloride ($FeCl_3.6H_2O$), Cobalt (II) chloride ($CoCl_2.6H_2O$), sodium hydroxide (NaOH), and pyridine were acquired from E. Merck Co., Germany and were used as received without further treatment.

2.2. Synthesis

2.2.1 Co-precipitation

The synthesis of the cobalt ferrite nanoparticles was prepared by the co-precipitating aqueous solutions of $CoCl_2$ and $FeCl_3$ mixtures in alkaline medium. Also the mixed solutions of $CoCl_2.6H_2O$ (100 ml, 1.0 M), and $FeCl_3.6H_2O$ (100 ml, 2.0 M) were prepared and kept at 60 °C.This mixture was added abruptly to the boiling solution of NaOH (1200 ml, 0.63 M). The solution was then stirred with constant velocity. After that, the solutions were maintained at 85 °C for 1h. This time duration was sufficient to form the spinel ferrite. A sufficient amount of fine particles was collected at this stage using magnetic separation. These nanoparticles were washed several times with distilled water followed by acetone and dried at room temperature [18].

2.2.2. Reverse micelles

In this study, the micro emulsion was used as the template for controlling the size of magnetic nanoparticles. The micro emulsion consists of three independent phases including petroleum oil, pyridine and partially polar species such as water or alcohol. To synthesize micro emulsion, briefly, pyridine is mixed with petroleum oil with volume ratio to ~1/10. After that, this mixture is then shaking vigorously to get partially emulsion mixture. This step takes time for ~1h. Then, the emulsion is refluxed at temperature to ~70 °C in an inert atmosphere of nitrogen for ~2h. Afterward, the emulsion is annealed until the temperature of the emulation reaches to room temperature.

In this reverse micelle, route is a triplet system of emulsion/ iso-butanol/H_2O was selected. For $CoFe_2O_4$ ferrite, aqueous solution was prepared by mixing stoichiometric amounts of 0.5 M of $FeCl_3$ and 0.25 M$CoCl_2.6H_2O$. Two reverse micro-emulsion "ME1" and "ME2" were prepared. 33.33 wt% of aqueous solution containing the precursor salts and 11.11 wt% of isobutanol, were then added to the oil under magnetic stirring. The stirring was continued for 1 h resulting in a stable reverse micro-emulsion ME1. Reverse micro-emulsion (ME2) was prepared with 4.0 M aqueous solution of NaOH as water phase under similar conditions.

The reverse micro-emulsion ME2 was then heated to 80 °C and to this was added reverse micro-emulsion ME1 dropwise under constant magnetic stirring. Appearance of blackish brown color after few minutes marks the completion of the reaction and formation of the desired ferrite colloidal solution. The reaction mixture was further stirred for 4 h on magnetic stirrer with temperature maintained at 80°C. At last, the synthesized nanoparticles were isolated by centrifugation and washed several times with distilled water, followed by ethanol, hexane and acetone by magnetic decantation. The final product was dried in air at 50 °C overnight to yield cobalt spinel ferrite nanoparticles.

2.3. Characterization

X-ray diffraction (XRD) patterns of the samples were recorded on a BRUKER X-ray powder diffractometer using Cu Kα (l 1.54060Å) radiation. The scans of the selected diffraction peaks were carried out in step mode (step size 0.02°, measurement time 2s, measurement temperature 25 °C, standard: Si powder).The lattice parameters and the site occupancy were determined by means of "Rietveld with energies" refinement[19], using the reflex program [20]. For the calculation of the crystallite size, "Scherrer's" method was applied [11]. After that, the crystallite size was refined by Rietveld refinement. The magnetic measurements of the prepared powder were determined at room temperature using the vibrating sample magnetometer (VSM, Dexing, Model: 250). The Fourier Transform Infrared Spectroscopy (FTIR) spectrum was recorded as (KBr) discs in the range 400–4000

cm^{-1} using the (FTIR–Shimadzu-8000) spectrophotometer.

3. Results and discussion

3.1. XRD analysis

Occasionally, the available powder diffraction data do not have enough information for a successful Rietveld refinement, for example for systems with a large number of degrees of freedom as occurring in all-atom refinements and/or for refinements using low quality powder data. In these cases, Rietveld refinements will typically lead to chemically unviable structures because the information content of the powder pattern is too low to determine accurately all the degrees of freedom.

To overcome this problem, Rietveld with energies allows you to incorporate an accurate description of potential energy in combination with the R_{wp} in the Rietveld refinement process, optimizing a combined figure of merit so as to not only the simulated pattern of the resulting structure matches the experimental diffraction data, but also the potential energy of the structure is not far off a global minimum. The aim is to find solutions that optimally meet two different and possibly conflicting objectives:

1- The simulated pattern has to match the experimental diffraction data.

2- The potential energy of the structure has to be close to the minimum [19-21].

The single-phase spinel nature of the powders, produced by the two different methods was confirmed by the X-ray diffraction pattern as shown in Fig. 1. The final product is $CoFe_2O_4$ with the expected inverse spinel structure and without any trace of impurity peaks. The unit cell symmetries can be described by the space groups $fd\overline{3}m$. The reflections are comparatively broader, revealing the nano-size of the crystals with the highest intensity and crystallinity in co-precipitation method [22].

To calculate the average grain size from the broadening of the XRD peaks of $CoFe_2O_4$, the "Rietveld with energies" refinement of XRD pattern was applied. The goodness of fit was tested by means of values of R_{wp}, whose values were below 10 %, indicating satisfied fit[20], as shown in Fig. 1. Table 1 shows the lists of crystallite size (D), lattice parameter (a), site occupancy, potential energy of crystal (E), and goodness of fit (R_{wp}, R_p, CMACS). There are major differences in the crystallite size and site occupation in the different preparation conditions, which give rise to different rates of ferrite formation, and favoring the variation in crystallite size. Furthermore, the micro-reactors in micro-emulsion not only simply control shape and size, but also decrease the aggregation process of crystals. Nevertheless, with respect to decreasing in site occupation of cobalt and iron ions and increasing in potential energy, we found out that crystalilinity in sample which was prepared by micro emulsion method was reduced [17].

However, TEM displays that the co-precipitation magnetic nanoparticles are spherical and roughly homogeneous in size (Fig.2). They are composed of ferrite aggregates having a diameter between 10 and 20 nm.

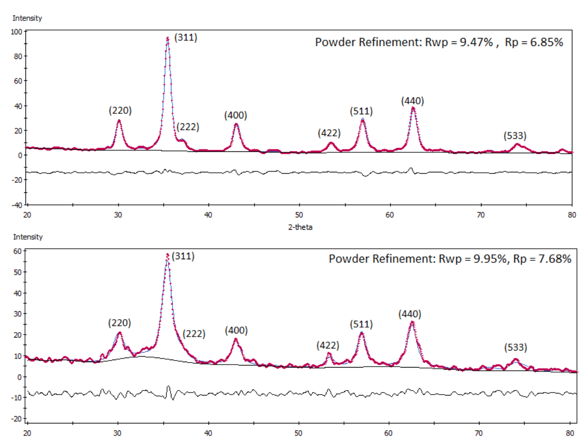

Fig. 1. XRD patterns of cobalt ferrite synthesis by (a) co-precipitation, (b) reverse micelles methods.

Table 1. crystallite size (D), lattice parameter (a), site occupancy, Energy (E), the weighted profile R-factor (R_{wp}),the profile R-factor (R_p), and Continuous Measure for the Automatic Comparison of Spectra (CMACS)

Synthetic method	D (nm)	a (nm)	site occupancy			E (kcal/mole)	R_{wp} (%)	R_p (%)	CMACS (%)
			Co	Fe	O				
Co-precipitation	12.02	0.8402	0.7931	0.9174	1.0000	833.34	9.47	6.85	1.38
Reverse micelles	7.07	0.8400	0.7526	0.8830	1.0000	835.42	9.95	7.68	2.43

3.2. FTIR analysis

Not simply is IR used to collect both to gather information about the structure of a compound, but it is also utilized as an analytical tool for assessing the purity of a compound. Fig. 3 exhibit the FTIR absorption bands of $CoFe_2O_4$ produced by co precipitation, micro-emulsion method at room temperature in the wave number range of 400–4000 cm^{-1}.

It is obvious that the higher frequency band (υ_1) is ~600 cm^{-1} and the lower frequency band (υ_2) is ~400 cm^{-1}. The bands υ_1 and υ_2 are related to the intrinsic vibration of tetrahedral and octahedral complexes [23]. The absorption bands, observed within this limit reveal the formation of the spinel structure.

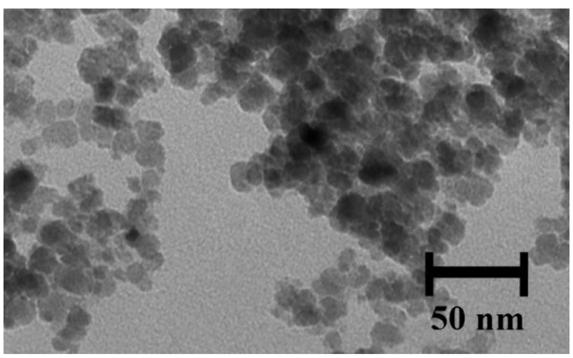

Fig. 2. TEM micrograph of cobalt nanoparticles prepared by co-precipitation method.

Two fundamental absorption bands appeared at 594cm^{-1} and 416 cm^{-1} for co-precipitation method, and at 594cm^{-1} and 393 cm^{-1} for reverse micelles.This difference in the band positions is observed because of the difference in the Fe^{3+}– O^{2-} distance and (1) the perturbation occurring, (2) introducing Co(II) ions for tetrahedral and octahedral sites.

The splitting of the octahedral ("B" site) absorption band near υ_2 is due to the presence of different kinds of cations including Co (II), Fe (III) and Fe (II) on the "B" site [24]. This is attributed to the "Jan–Teller" distortion produced by Fe (II) ions, which produces the local deformation in the crystal field potential, thereby splitting the absorption band [25].

The magnetic properties of materials originate from the quantum couplings at the atomic level, including the coupling between electron spins (S-S coupling) and the coupling between the electron spin and the angular momentum of the electron orbital (L-S coupling).[26] Each of the magnetic nanoparticles tends to possess a single magnetic domain. Therefore, the nanoparticles provide excellent opportunities for the fundamental studies on the relationship between magnetic behavior and the magnetic couplings at the atomic level. The magnetization curves of the cobalt ferrite.

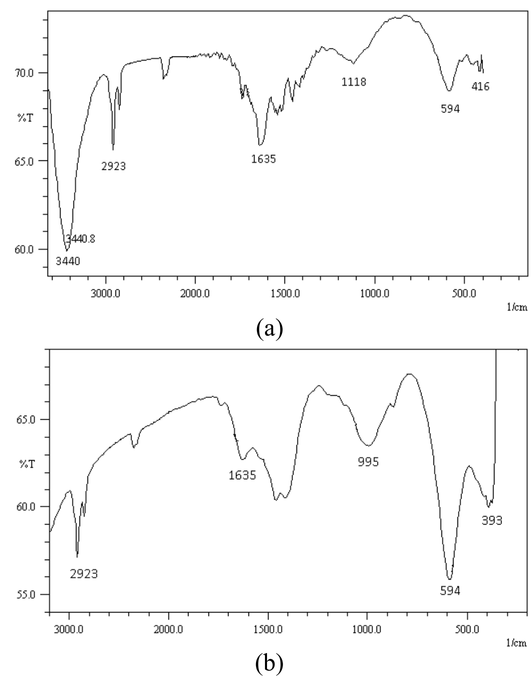

Fig. 3. FT-IR spectra of the cobalt ferrite synthesis by (a) co-precipitation, (b) reverse micelles methods.

3.3. Magnetic properties

Nanoparticles measured at 27 °C are shown in Fig. 4. It is clear that, the synthesis method can influence the magnetization curves because of a change in the particle size and crystallinity.

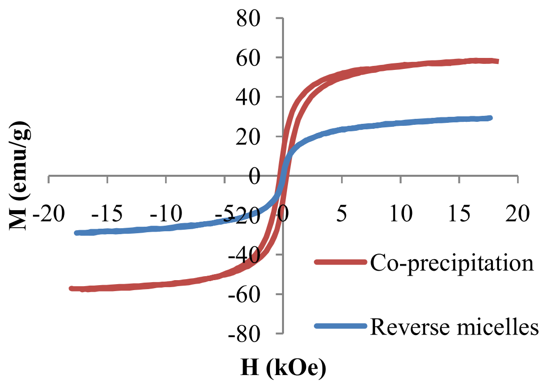

Fig. 4. M-H curves of different prepared samples

3.3.1. Saturation Magnetization

Table 2 illustrates the dependence of the saturation magnetization on the synthesis method. The M_S value obtained for the samples is different from the bulk value of 80.8 emu g^{-1} at room temperature for $CoFe_2O_4$ [25]. The higher M_S in the co-precipitation method is mainly due to the larger particle sizes and is slightly due to the higher crystallinity.

Table 2. Saturation magnetization, coercivity, remainance, maximum magnetic field and canted layer thickness measured at 27 °C

Synthetic method	M_S(emu g^{-1})	H_C(Oe)	M_r(emu g^{-1})	H_{max}(kOe)	t_{shell}(nm)
Co-precipitation	58.4	286.0	12.45	18.0	0.74
Reverse micelles	29.4	25.2	0.84	17.6	0.87

The existence of some degree of the spin canting in the whole volume of the nanoparticles, the disordered surface/dead layer and the spin-glass properties at the surface can explain the decrease of the saturation magnetization. The dead magnetic layer originates from the demagnetization of the surface spin causes the surface spins to be disordered or misaligned. It also leads to the super-exchange interaction between the Fe-O-Fe bonds, caused by termination of the bonds. It phenomenon weakens the total magnetization of the nanoparticles [26]. The dead layer thickness (t) of spherical nanoparticles can be calculated by (Eq. 1) [25]. Where, "D" is the particle size, M_{sat} is the saturation magnetization and $M_{sat\text{-}0}$ is the saturation magnetization at 0 K. The saturated magnetizations are about 80.8 emu g^{-1} and 93.9 emu g^{-1} at room temperature and 5 K, respectively [25]. From Table 2, it is clear that, the dead layers depend not only on the particle size, but also on the saturation magnetization to the size ratio.

$$M_{sat} = M_{sat\text{-}0}\,(1 - 6t/D) \qquad (1)$$

3.3.2. Magnetic coercivity (H_C)

The magnetic coercivity of the nanoparticles depends significantly on their magneto-crystalline anisotropy, micro-strain, inter-particle interaction, temperature, size and shape.[26] In the $CoFe_2O_4$ spinel, the Co(II) ($3d^7$, $4F_{9/2}$, L=3, S=3/2, J=9/2) cations have high spin ligand fields and possess seven d electrons three of which are unpaired. Evidently, the large magneto-crystalline anisotropy E_A of $CoFe_2O_4$ nanoparticles is due to the strong L-S couplings on the Co (II) cation sites. This effect results in the nanoparticles with multi-axial anisotropy, and the zero coercivity can be achieved at very low particle sizes (2-3 nm) [27].

Table 2 lists the magnetic coercivity and magnetic remainance for nanoparticles obtained from two different synthesis methods with a uniform composition. The results revealed that by changing the method from co-precipitation to the reverse micelle the material exhibits a softer magnetic behavior in such a way that magnetic coercivity decrease from 286 Oe for co-precipitation to 25.2 Oe for the reverse micelle methods.

4. Conclusions

In this paper, $CoFe_2O_4$ powders were synthesized by two methods, including co-precipitation, and reverse micelle methods with one starting material/uniform chemical composition. The data obtained from XRD, FTIR and VSM revealed that:

1. The particle size has strong effect on the magnetic properties and also the size effect can cover the role of slight crystallinity.

2. The nanoparticles, synthesized by the co-precipitation method have larger particle sizes, higher crystallinity, saturation magnetization and coercivity, as compared to the micelles method.

3. The nano crystalline $CoFe_2O_4$ shows the absorption bands ~600 and 400 cm^{-1}, respectively. The high frequency band ν_1 around 600 cm^{-1} is attributed to the tetrahedral complexes and the band υ_2 ~400 cm^{-1} corresponds to the octahedral complexes.

4. The magnetic properties of the sample strongly depend on the size of the nanoparticles.

5. This research work investigates the effect of two widely used wet chemical methods including co-precipitation, and reverse micelles.

References

1. Neel, L., Ann. *Geophys*., Vol. 5 (1949) 99.
2. Frankel, J., Dorfman, J., *Nature, Vol.* 126, p. 274, 1930; Kittel, C., *Phys. Rev., Vol.* 70 (1946) 965.
3. Maria, G. B. S., Antipina, N., *Adv Drug Deliv. Rev.,* Vol. 63 (2011) pp. 716-29.
4. Kai Zhang, T. H., Pradhan, A. K*., J. Magn. Magn. Mater*., Vol. 323 (2011) pp. 1616-22.
5. Shokrollahi, H., Janghorban, K., *Mater. Sci. Eng.* B, Vol. 141 (2007) pp. 91-107.
6. Shokrollahi, H*., J. Magn. Magn. Mater*., Vol. 320 (2008) pp. 463-474.
7. El-Shobaky, G. A., Turky, A. M., Mostafa, N. Y., Mohamed, S. K., *J. Alloys Compd*., Vol. 493 (2010) pp. 415-22.
8. Ahmed, M. A., EL-Khawlani, A. A., *J. Magn. Magn. Mater., Vol.* 321 (2009) pp. 1959-63.
9. Rana, S., Philip, J., Raj, B., *Mater. Chem. Phys., Vol.* 124 (2010) pp. 264-69.
10. Ayyappan, S., Mahadevan, S., Chandramohan, P., Srinivasan, M. P., Philip, J., and Raj, B., *J. Phys. Chem. C,* Vol. 114 (2010) pp. 6334-41.
11. Yousefi, M. H., Manouchehri, S., Arab, A., Mozaffari, M., Amiri, G. R., Amighian, J., *Mater. Res. Bull., Vol.* 45 (2010) pp. 1792-95.
12. Dave, S. R., Gao, X., *Monodisperse magnetic nanoparticles for biodetection, imaging, and drug delivery: a versatile and evolving technology,* John Wiley & Sons, Inc. 1, (2009).
13. R. Arulmurugan, B. Jeyadevan, G. Vaidyanathan, S. Sendhilnathan, *J. Magn. Magn. Mater*., Vol. 288 (2005) pp. 470-477.
14. Zi, Zh., Sun, Y., Zhu, X., Yang, Zh., Dai, J., Song, W., *J. Magn. Magn. Mater.,* Vol. 321 (2009) pp. 1251-55.
15. Pileni, M. P., *J. Phys. Chem.,* Vol. 97 (1993) pp. 6961-73.
16. Mahmoudi, M., Sant, Sh., Wang, B., Laurent, S., Sen, T., *Adv. Drug Deliv. Rev.,* Vol. 63 (2011) pp. 24-46.
17. Lo´pez-Quintela, M. A., Tojo, C., Blanco, M. C., Garcı´a Rio, L., Leis, J. R., *Curr. Opin. Colloid Interface Sci.,* Vol. 9 (2004) pp. 264-78.
18. Vaidyanathan, G., Sendhilnathan, S., Arulmurugan, R., *J. Magn. Magn. Mater., Vol.* 313 (2007) pp. 293-299.
19. Rietveld, H., *J. Appl. Crystallogr.,* Vol. 2 (1969) pp. 65-71.
20. Young, R. A., *The Rietveld Method*, Oxford University Press, 1993.
21. Veldhuinzen, D. A. Van, Lamont, G. B., *Evolutionary Computation*, Vol. 8 (2000) pp. 125-47.
22. Kumar, S., Singh, V., Aggarwal, S., Mandal, U. K., Kotnala, R. K., *J. Phys. Chem.* C, Vol. 114 (2010) pp. 6272-80.
23. Waldron, R. D., *Phys. Rev.*, Vol. 99 (1955) pp. 1727-35.
24. Trivedi U. N., Jani, K. H., Modi, K. B., Joshi, H. H*., J. Mater. Sci. Lett.,* Vol. 19 (2000) pp. 1271-73.
25. Tung, L. D., Kolesnichenko, V., Caruntu, D., Chou, N. H., O'Connor, C. J., and Spinu, L., *J. Appl. Phys.,* Vol. 93 (2003) pp. 7486-88.
26. Caizer, C., Stefanescu, M., *J. Phys. D: Appl. Phys*., Vol. 35 (2002) pp. 3035-40.